Dynamics of radio-emitting electrons in the Cygnus A cavity: boundary backflow; complex hotspot structure; first computation of sync. emission throughout cavity; demonstration that jets and cavity are relativistic electron-pairs

Bill Mathews

University of California, Santa Cruz

for Galaxy Formation Workshop 2013

former collaborator: Fulai Guo (ETH Zurich)

Chandra X-ray image of Cygnus A

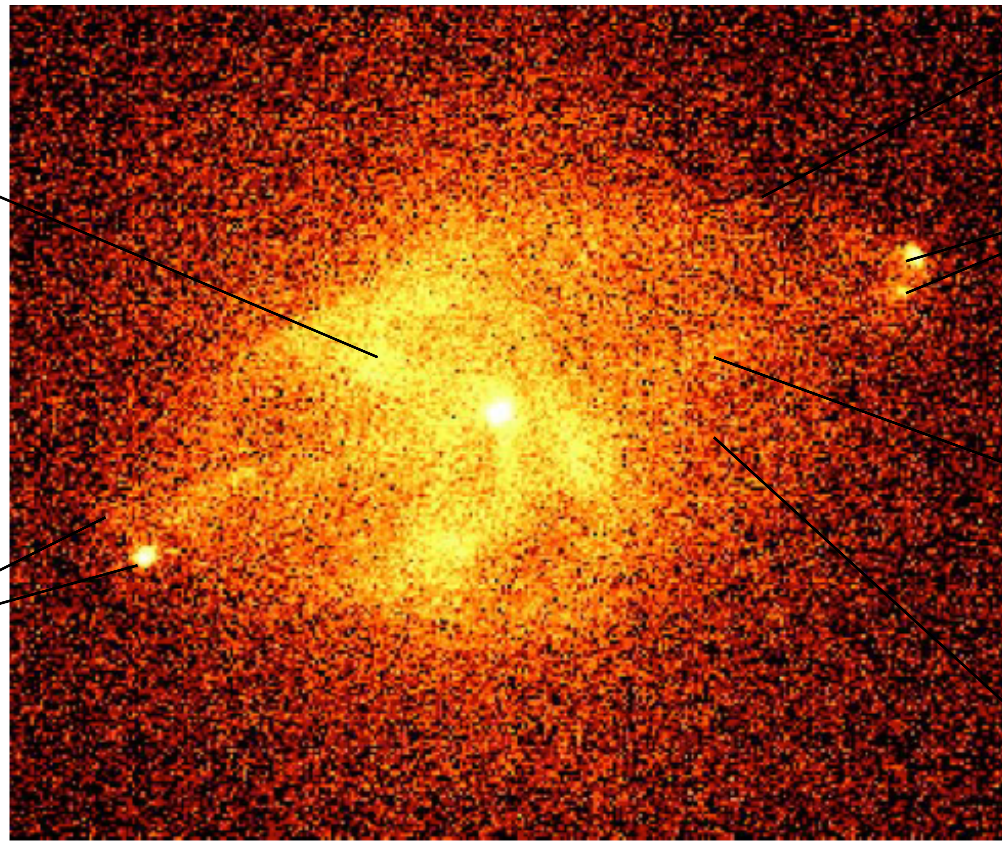

Wilson+06

located at center of cluster of mass ~10^{15} M_{sun}

Cygnus A is a classic FRII double lobe radio source

age of Cygnus A event is ~10^7 yrs
from sync. losses
Mach no. of bow shock

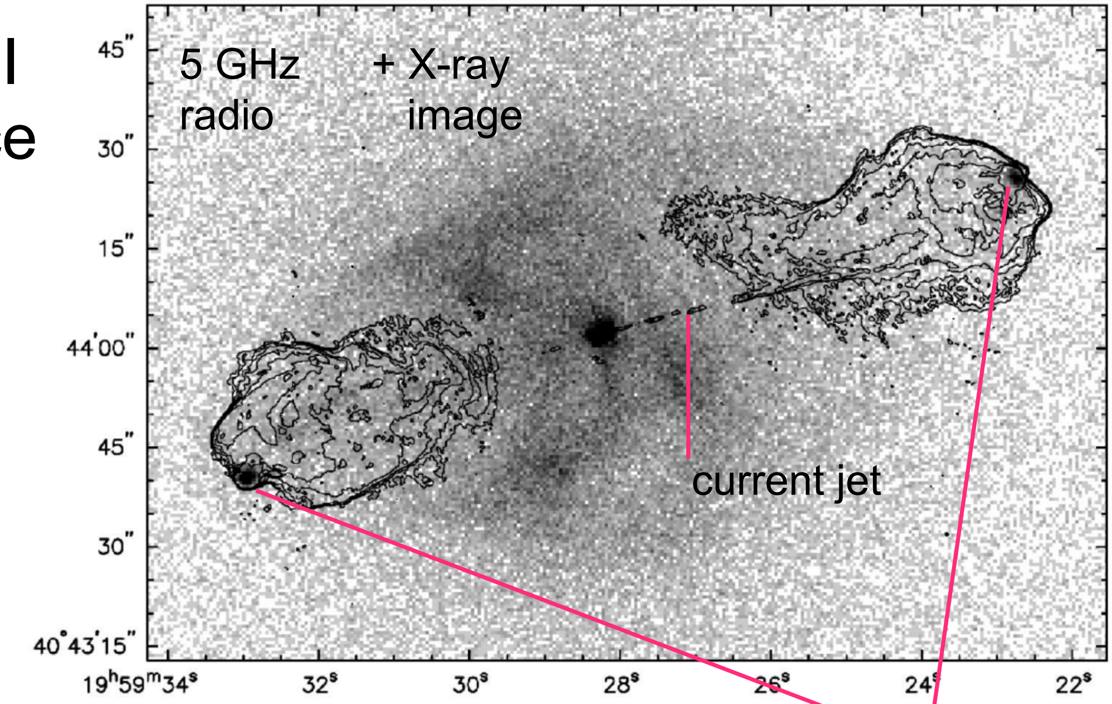

radio hotspots

jet volume is small -- no hotspot yet

high energy CRes emit at high-ν closer to hotspot

1 15 GHz
2 8
3 5
4 1.34
5 0.33
6 0.15

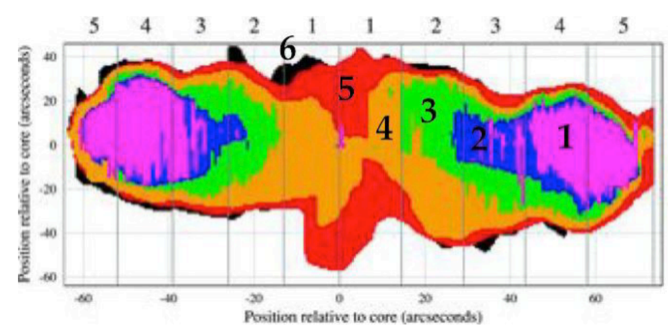

6 radio images super-imposed

well-ordered radio electron ages

three most recent jet-driven FRII lobe calculations

2D hydro

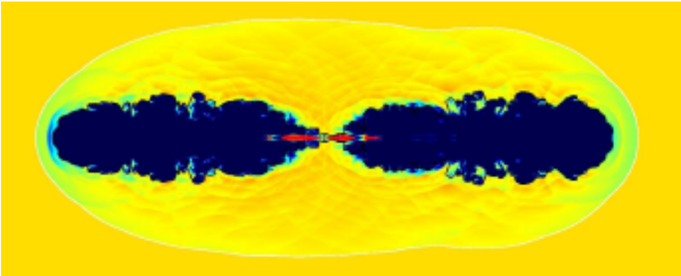

2013

3D MHD

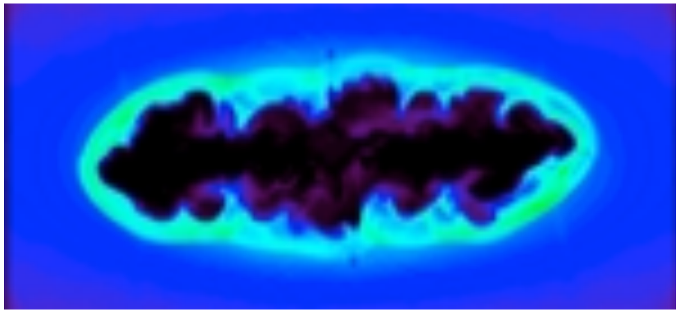

2011

3D MHD

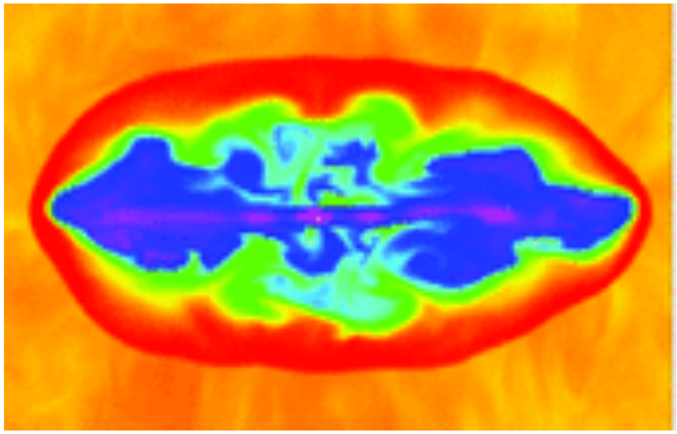

2011

radio cavities are dynamically chaotic

radio electron ages will be mixed

it's time for a more realistic computation!

2D axisymmetric computations with a relativistic component

gas: $P = (\gamma - 1)e \quad \gamma = 5/3$

CRs: $P_c = (\gamma_c - 1)e_c \quad \gamma_c = 4/3$

$$\frac{\partial \rho}{\partial t} + \nabla \cdot \rho \mathbf{u} = 0$$

$$\rho\left(\frac{\partial \mathbf{u}}{\partial t} + (\mathbf{u}\cdot\nabla)\mathbf{u}\right) = -\nabla(P + P_c) - \rho\nabla\Phi$$

$$+ \nabla \cdot \mathbf{\Pi} + \frac{1}{4\pi}(\nabla \times \mathbf{B}) \times \mathbf{B}$$

viscous force

ignore Lorentz force: observe $B^2/8\pi << e_c$

thermal energy density

$$\frac{\partial e}{\partial t} + \nabla \cdot \mathbf{u}e = -P(\nabla \cdot \mathbf{u}) - \mathcal{L}_{rad} + \mathbf{\Pi} : \nabla\mathbf{u}$$

ignore radiation losses: small during t_{age} ~10^7 yrs

viscous dissipation

CR energy density*

$$\boxed{\frac{\partial e_c}{\partial t} + \nabla \cdot \mathbf{u}e_c = -P_c(\nabla \cdot \mathbf{u})} + \nabla \cdot (\kappa \nabla e_c)$$

ignore CR diffusion: small during t_{age} if κ ~10^{28} cm^2/s as in Milky Way also: no age mixing

passive frozen-in field

$$\frac{\partial \mathbf{B}}{\partial t} = \nabla \times (\mathbf{u} \times \mathbf{B}) \qquad \nabla \cdot \mathbf{B} = 0$$

*expect $P_c > P$

CR age

$$\boxed{\frac{\partial \tau}{\partial t} + \nabla \cdot \tau\mathbf{u} = 0} \quad \tau = \rho t_{exss} \quad t_{age}(r, z) = 10 - \tau/\rho \;\; \text{Myrs}$$

radio polarization observations

hotspot field appears ~ toroidal

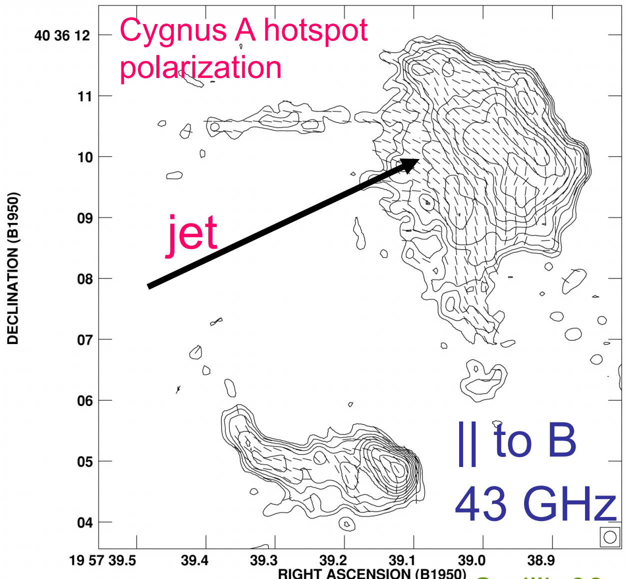

Carilli+99

but non-toroidal fields appear downstream

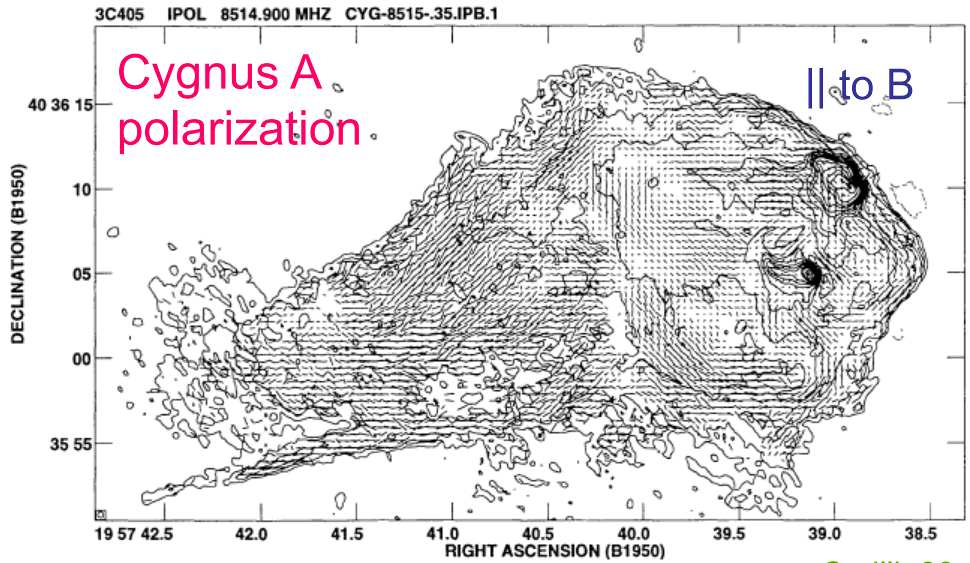

Carilli+99

assume a <u>shockspot-driven flow</u>: jet is not explicitly computed

this is OK since:

faint jet occupies a <u>negligible volume</u>

<u>at each time step</u> moving shockspot is injected with

(1) 10^{46} erg/s of relativistic CRs to fill Cygnus A radio cavity volume in 10^7 yrs

(2) 1 M_{sun}/year of non-relativistic gas with v_{ss} -- for B to freeze onto

(3) toroidal hotspot field is reset to constant value: e. g. B_{ss} ~ 100 μG

assume field, cosmic rays and gas in radio cavity all originate in a moving "<u>shockspot</u>" where the jet terminates

shockspot source zones move along the grid z-axis at constant velocity v_{ss}:

v_{ss} = 60kpc/10^7yrs = 5800 km/s

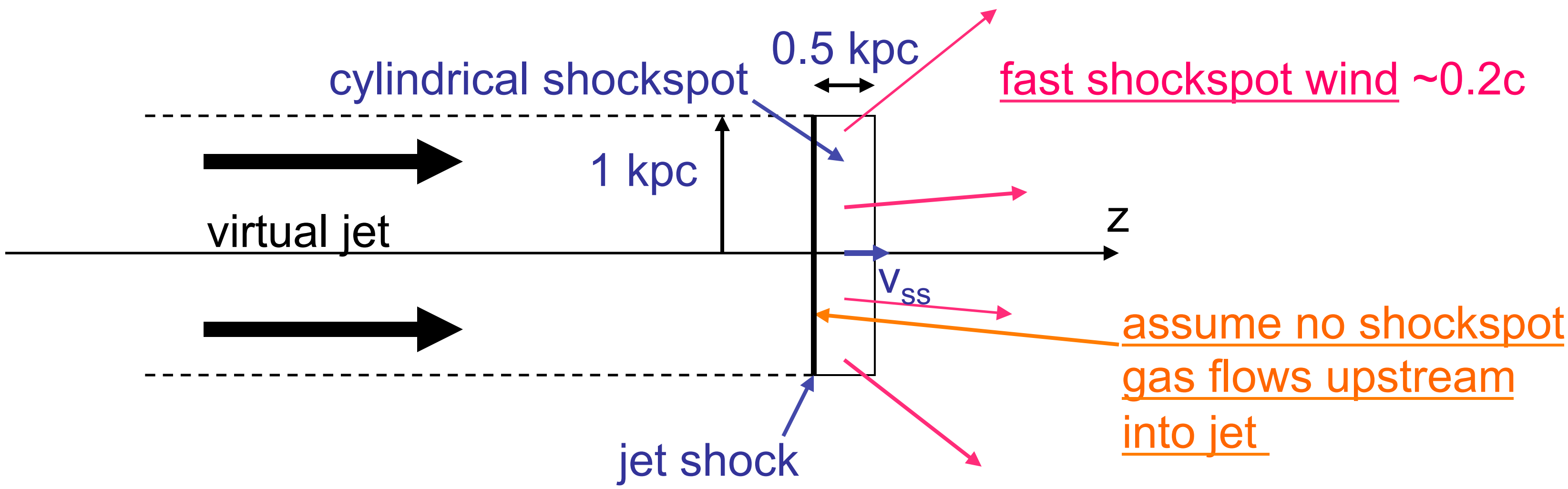

assume a purely <u>toroidal field ($B = B_\theta$)</u>

toroidal fields automatically satisfy divB = 0
as they flow from the shockspot

<u>poloidal fields</u> (B_r, B_z) cannot be used in moving shockspot sources without violating divB = 0 – true for all common MHD codes (“constrained transport”)

after 10^7 yrs:

density

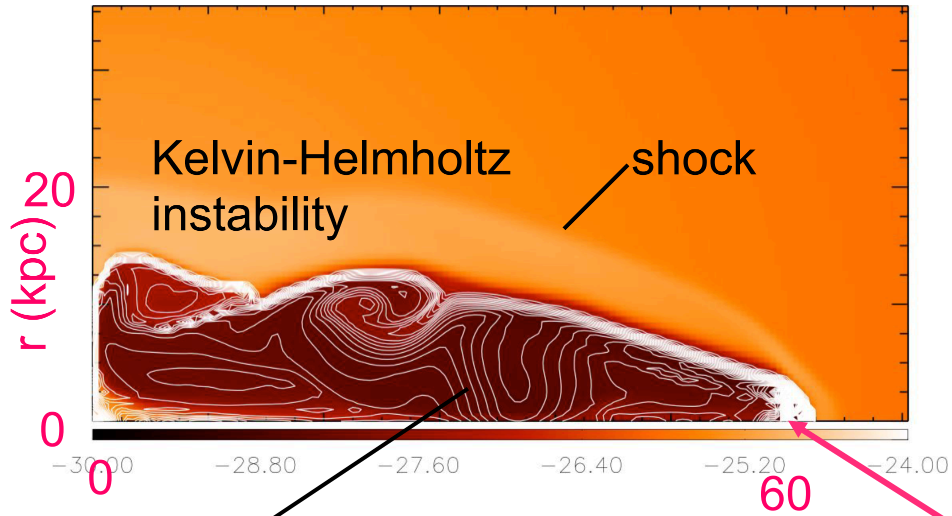

radio cavity

shockspot

gas density with
CR energy density
contours

velocity

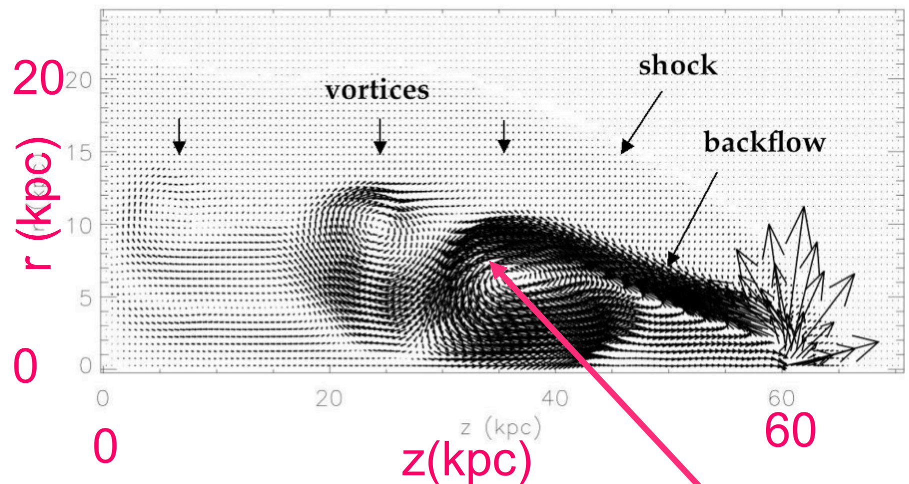

<u>boundary backflow</u>
disturbed by <u>internal</u>
KH vortices

Kelvin Helmholtz instability
first occurs inside cavity,
not at cavity boundary

density

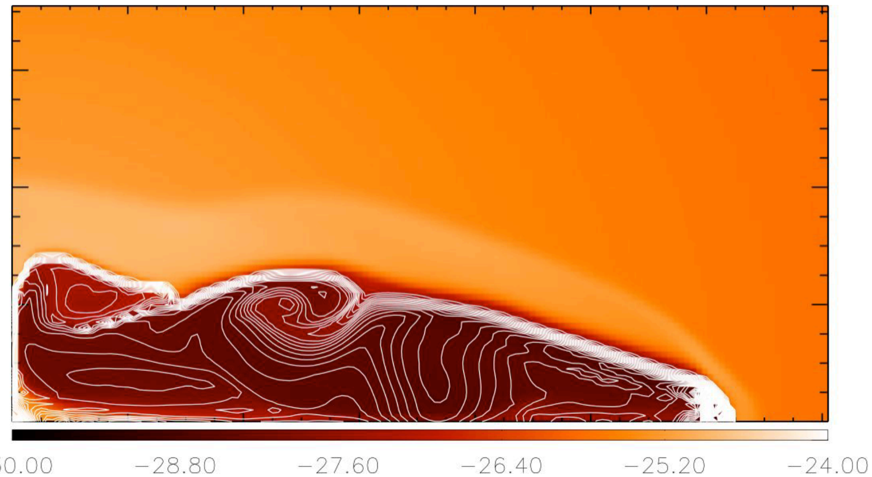

velocity

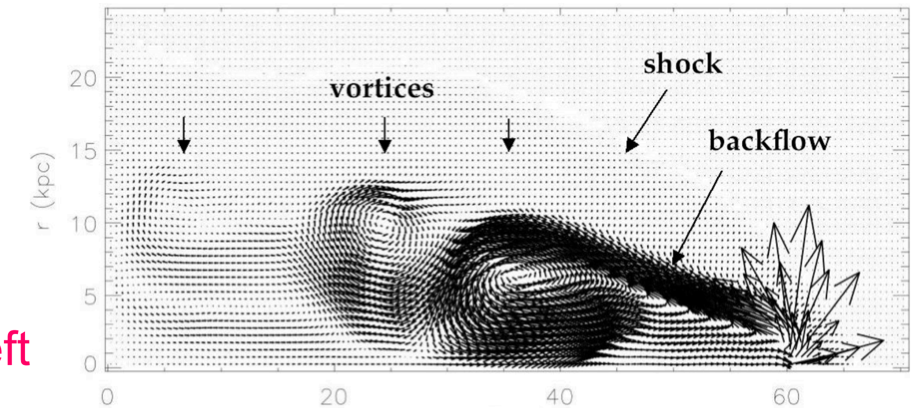

advect time CRs left shockspot t_{ss}

projected CR age 10 - t_{ss} weighted along los by synchrotron emission

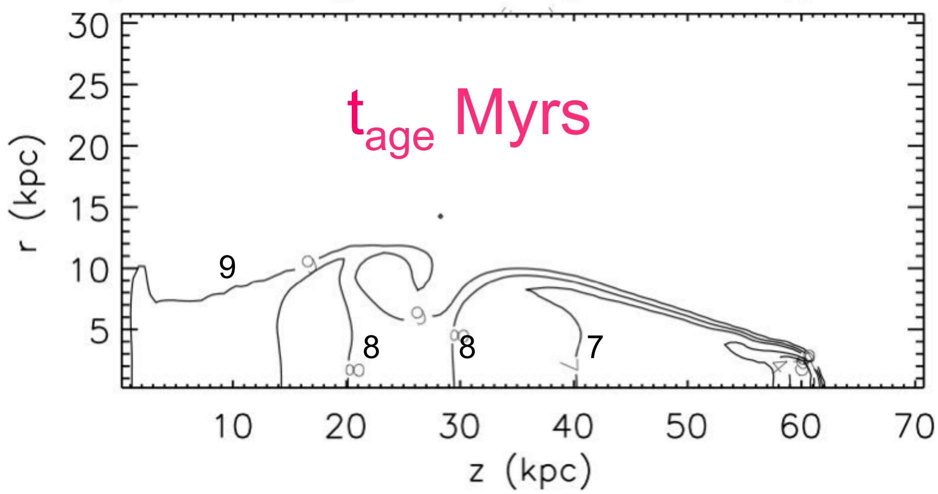

projected sync. age is <u>not monotonic</u> as in Cygnus A

Must stop KH with (huge) B or viscosity…

Repeat with viscosity
$t = 10^7$ yrs

density

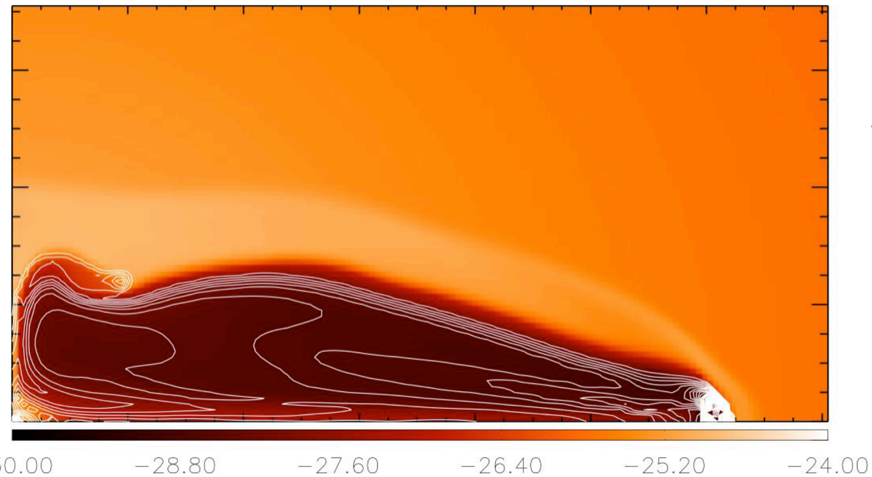

KH is suppressed with small viscosity
$\mu = 30$ gm/(cm s)

velocity

backflowing CRs decelerate rapidly (due to $dP_c/dz<0$), increasing B

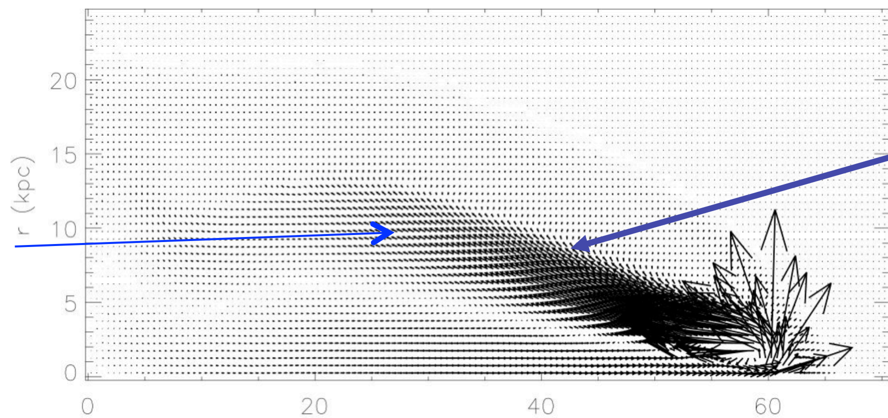

first computation of smooth boundary backflow!

projected
CR age 10 - t_{ss}
weighted
along los
by synchrotron
emission
(toroidal field)

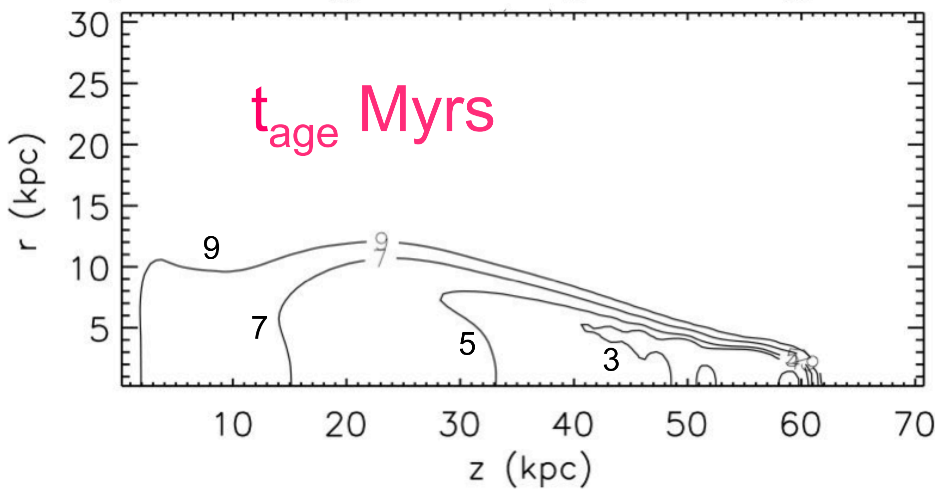

now CR age varies monotonically as in Cygnus A

synchrotron emission from computed boundary backflow

sync. surface brightness $\int e_c u_B \, ds$

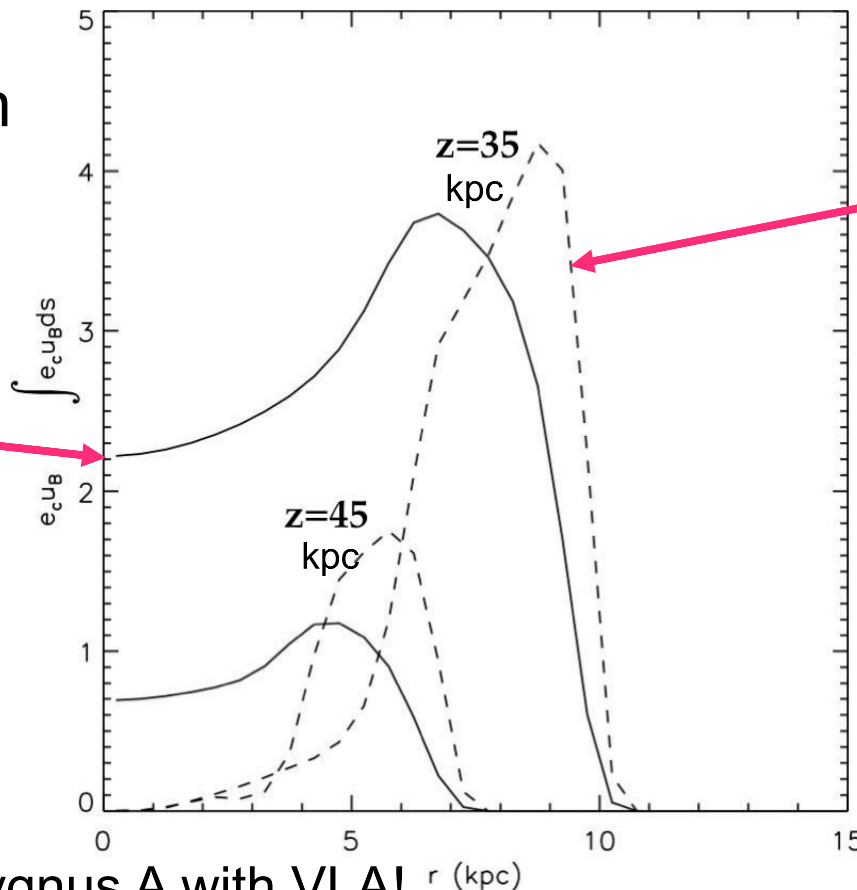

$e_c u_B$ (proxy for sync. emissivity) peaks at radio lobe boundary

$$\boxed{u_B = \frac{B^2}{8\pi}}$$

is observed in Cygnus A with VLA!

z kpc from center

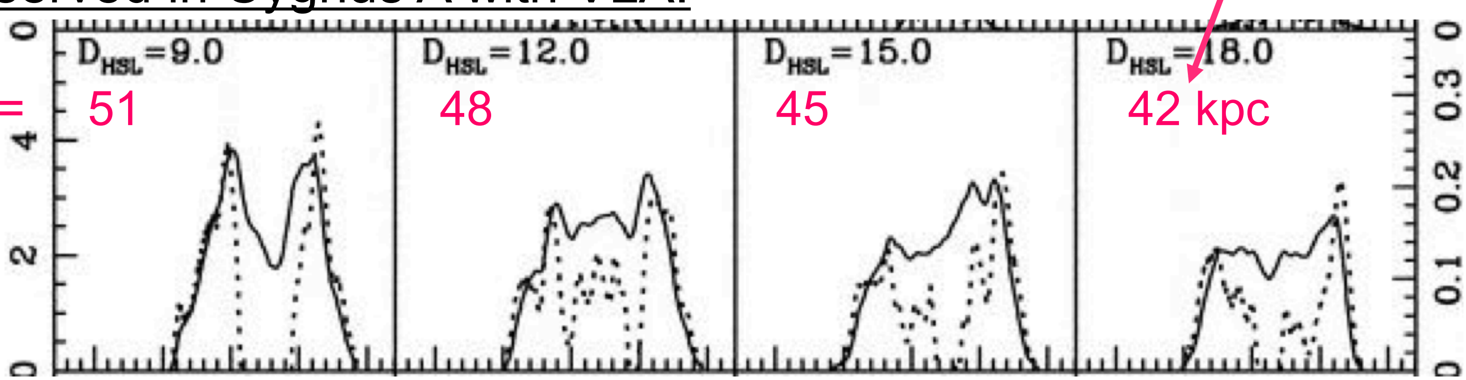

-20 0 20
arcsec (kpc)

Carvalho+05

1.3GHz

radio emission from active FRII radio lobes
comes from boundary backflow; very limb-brightened

similar to γ-ray IC-CMB emission in the Fermi bubbles for first time: can connect observed B_{ss} and $B_{backflow}$

a toroidal field increases in decelerating flow $u_z \perp B$

radio lobe
CR pressure
is nearly
uniform

$3P_c$

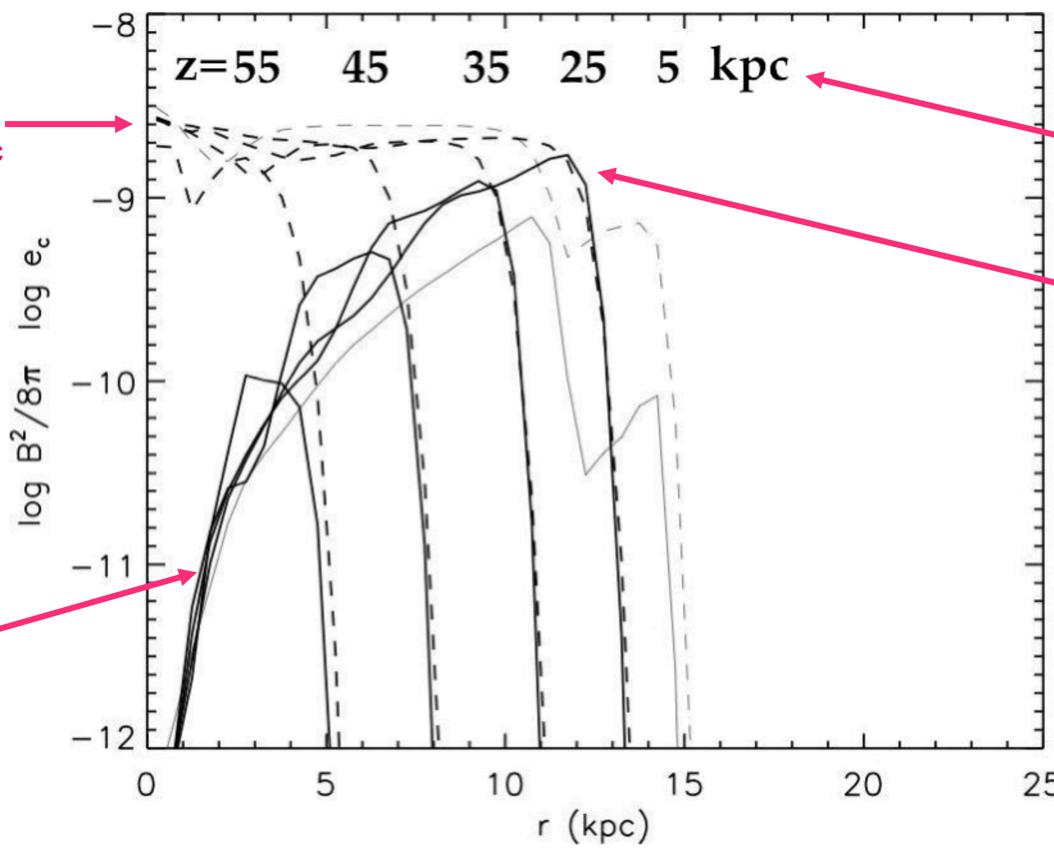

kpc from
center

backflowing
field

$\frac{B^2}{8\pi}$

backflowing toroidal magnetic field Is ~20X too large and the computed radio emissivity $e_c u_B$ increases along decelerating boundary backflow

but observed radio emissivity observed in Cygnus A
decreases along boundary backflow

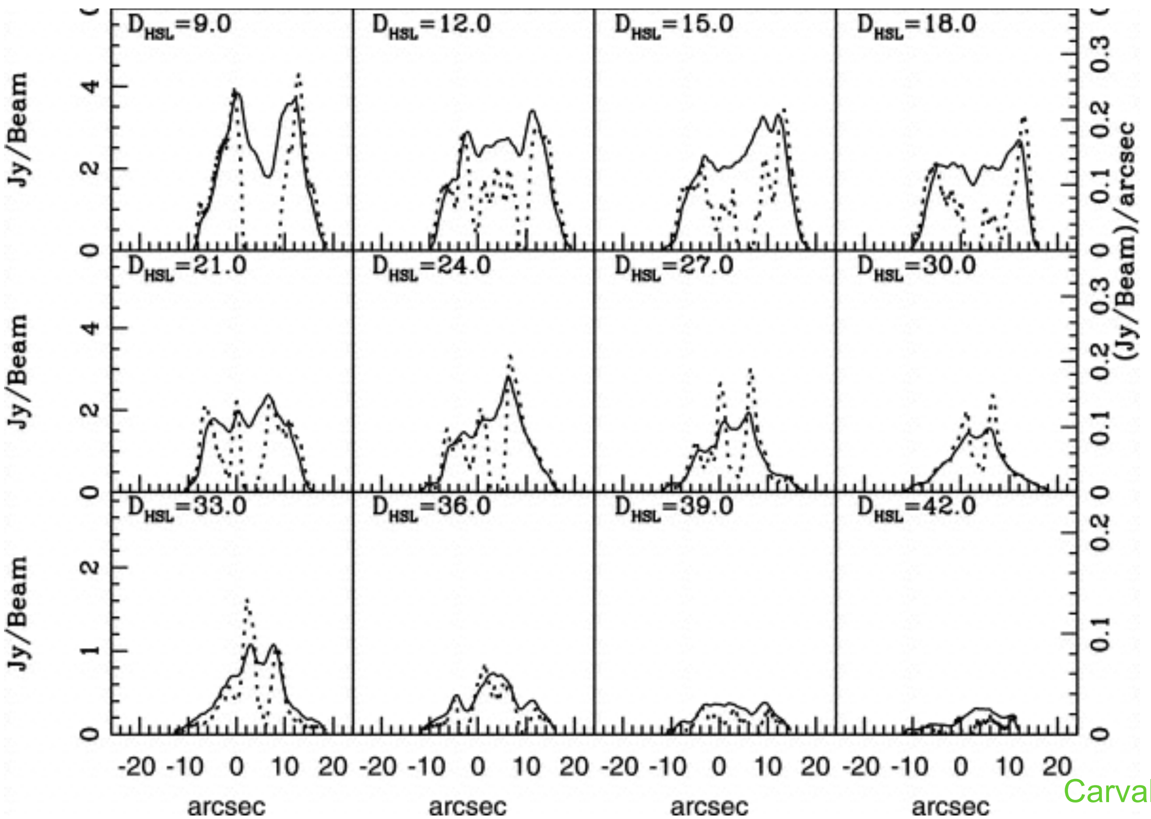

1.3GHz

Carvalho+05

Solutions with toroidal magnetic field are unlike observations

non-thermal radio and X-ray emission near hotspot

<u>B in shockspot wind grows exponentially</u>
as wind decelerates and compresses against dense (shocked) cluster gas ahead

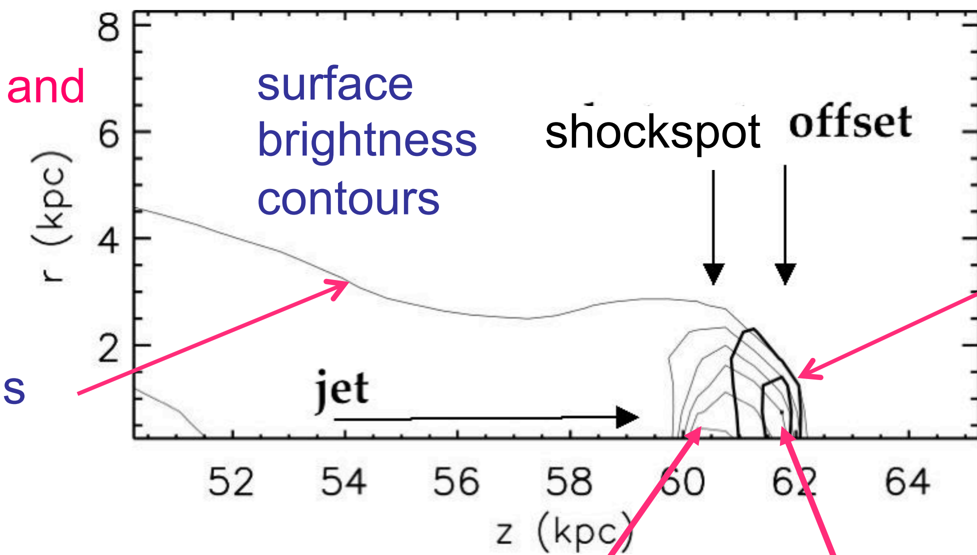

$\int e_c\, u_{cmb}\, ds$

$\int e_c\, u_B\, ds$

SHOCKSPOT

OFFSET BRIGHTSPOT

weak radio sync.
$\int e_c\, u_B\, ds \quad << \quad \int e_c u_B\, ds$

strong radio sync.

strong X-ray
synchroton self-Compton (SSC)
$\int e_c u_{sy}\, ds \qquad u_{sy} \sim L_{sy}(r/c)/V$

the brightest radio & X-ray emission is
<u>not from the shockspot</u>
but from the arc-shaped offset compression ~1.5 kpc ahead

compare the incredibly powerful FRII hotspot in 4C74.26

500 kpc from its cluster center   can observe both shockspot and offset

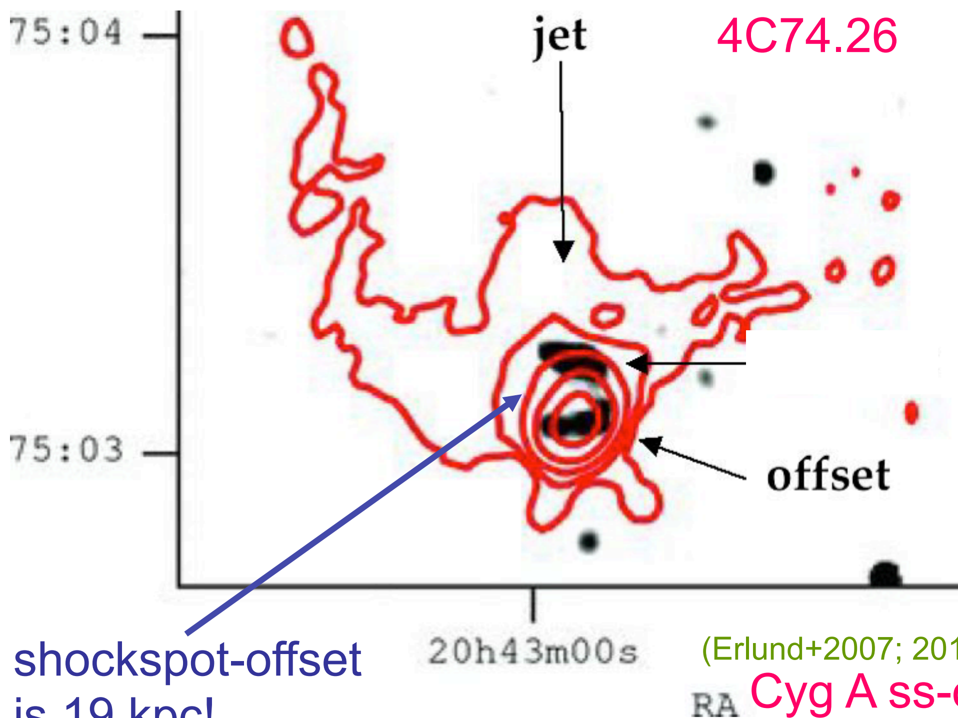

Red contours: radio observations 1.4GHz

Grey scale: X-ray image

X-ray sync. emission from shockspot?

radio sync. & X-ray SSC
from arc-shaped offset

shockspot-offset
is 19 kpc!

(Erlund+2007; 2010)

Cyg A ss-offset increases as cluster ρ decreases:

radio

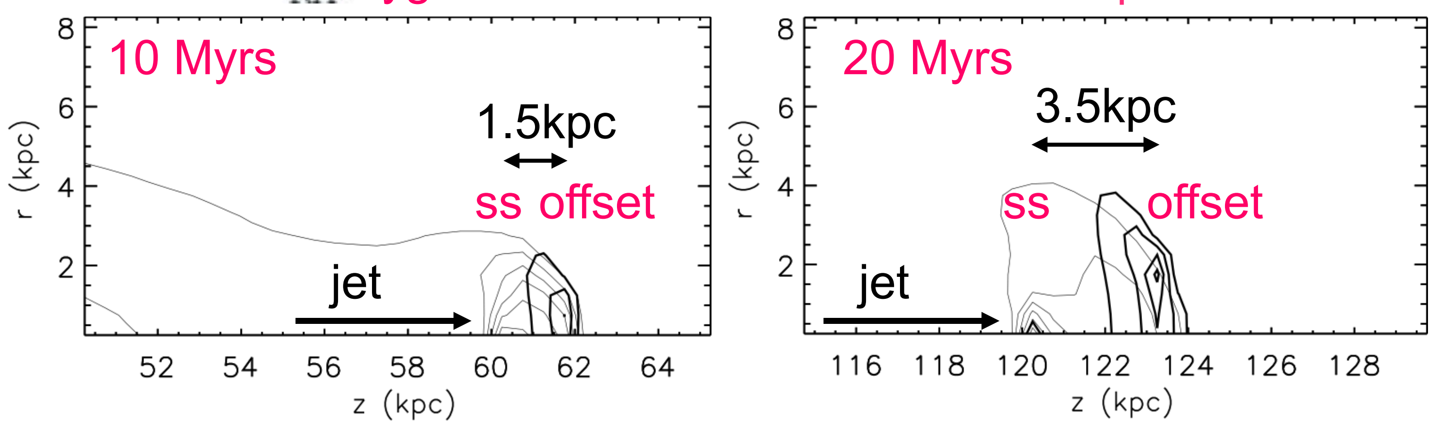

subsonic communication determines shockspot-offset distance

consider 1D flow along jet direction

Mach number in frame of cavity-cluster contact discontinuity $u_z(z_{cd})$

$$\mathcal{M} = \frac{u_z(z) - u_z(z_{cd})}{c_s} < 1$$

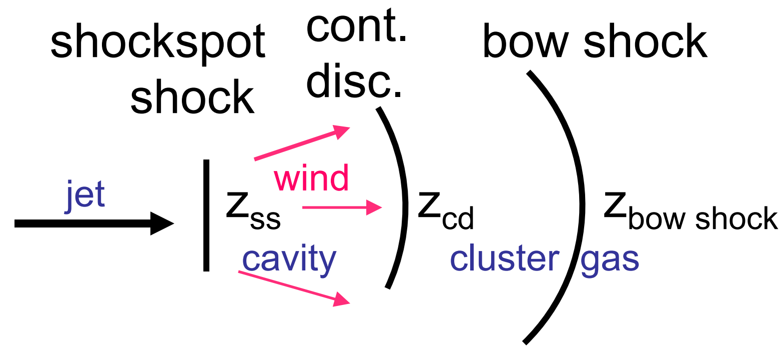

is subsonic between the shockspot and cluster gas bow shock.

in our calculation the shockspot is required to move at constant velocity, but

- in reality the shockspot shock can back off from the cavity boundary until the recoil momentum of the shockspot wind balances the jet momentum

some conclusions of shockspot-driven FRII evolution:

- KH instabilities inside the radio lobe must be damped
  to reproduce smooth radial variation of radio electron ages
  viscous damping more likely than magnetic damping
- radio synchrotron emission occurs in a narrow boundary backflow.
  sync. emission in active radio lobes is limb-bright – as observed
- the bright radio-X-ray "hotspots" in Cygnus A
  are offset emission ahead of the post-shock shockspot
  brightest radio sync. and X-ray SSC emission
  occurs as shockspot wind compresses against cluster gas
- Toroidal shockspot fields
  evolve into lobe fields much larger than observed
  sync. em. Increases along backflow – not observed
- computed flow is subsonic between shockspot and cluster bow shock,
  allowing the shockspot-offset distance to adjust to the jet momentum

recent developments:

- new terminology for "hotspot" structure:
  "shockspot" (ss): region just behind jet shock, origin of cavity wind
  "bright spot" (bs): luminous region where wind impacts cluster gas

- accurate estimates of evolution of CR electron energy distribution $n(\gamma,\mathbf{r},t)$ from ss to radio cavity of Cygnus A

- accurate estimates of evolution of radio synchrotron emissivity ε_ν and flux from the radio cavity

- results support random, small-scale magnetic field inside cavity

★ electron pairs dominate Cygnus A jet and cavity synchrotron emission evolution of synchrotron electrons from shockspot to cavity

electron energy distribution

$n(\gamma,\mathbf{r},t)$

$$\boxed{\frac{\partial n}{\partial t} + \nabla \cdot n\mathbf{u} = \frac{\partial}{\partial \gamma}\left[-\dot{\gamma} n\right]}$$

assume uniform expansion

$$\nabla \cdot n\mathbf{u} \approx n\nabla \cdot \mathbf{u} = n(3/t)$$

$n(\gamma,\mathbf{r},t) = n(\gamma,t)$

with expansion + sync. losses

$$\dot{\gamma} = -\left(\frac{\gamma}{t} + \frac{\gamma^2}{t_*}\right)$$

$$\frac{1}{t_*} = \frac{4}{3}\frac{\sigma_T}{m_e c}\left(u_{cmb} + \frac{2}{3}\frac{B^2}{8\pi}\right)$$

equation for n(γ,t):

$$\frac{\partial n}{\partial t} - \left(\frac{\gamma}{t} + \frac{\gamma^2}{t_*}\right)\frac{\partial n}{\partial \gamma} = 2\left(\frac{\gamma}{t_*} - \frac{1}{t}\right) n$$

initial power law in ss:

$$n(\gamma, t_0) = K\gamma^{-p}$$

particular solution:

expansion radiation

$$n(\gamma, t) = K\gamma^{-p}\left(\frac{t}{t_0}\right)^{-(2+p)}\left[1 - \left(\frac{\gamma t_0}{t_*}\right)\left(\frac{t}{t_0}\right)\ln\left(\frac{t}{t_0}\right)\right]^{p-2}$$

$$\rho \propto t^{-3} \qquad e_c \propto \rho^{4/3} \propto t^{-4} \qquad \left(\frac{t}{t_0}\right) = \left(\frac{e_c}{e_{c,ss}}\right)^{-1/4}$$

computed variation of e_c and gas density in shockspot:

$e_{c,ss}$

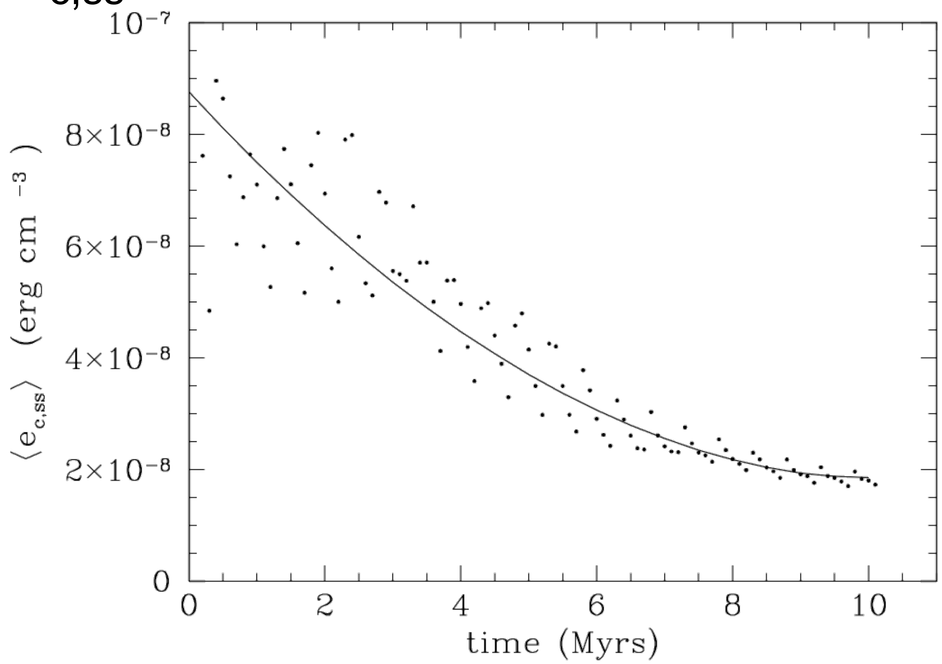

time

$\rho_{c,ss}$

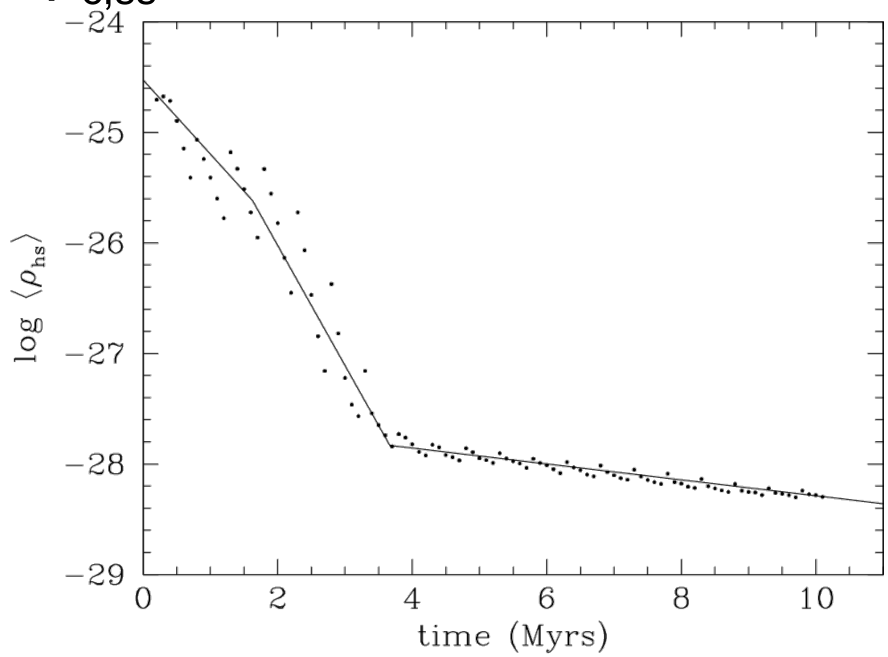

time

correct observations of bs to the ss using hydro results:

observations of Cygnus A brightspot – a double power law:

$$n(\gamma) = \min[n_1(\gamma), n_2(\gamma)]$$

where

$$n_1(\gamma) = K\gamma^{-p_1} \quad \text{for} \quad \gamma < \gamma_{cr}$$

$$n_2(\gamma) = K\gamma_{cr}^{p_2-p_1}\gamma^{-p_2} \quad \text{for} \quad \gamma > \gamma_{cr}$$

$$p_1 = 1.5,\ p_2 = 3.3,\ \gamma_{cr} = 2000$$
$$K = K_{bs} = 1.1 \times 10^{-4}\ \text{cm}^{-3}$$

(Stawarz+07)

correction from brightspot to shockspot values:

$$K_{ss} = (e_{c,ss}/e_{c,bs})K_{bs} = 1.38K_{bs} = 1.49 \times 10^{-4}\ \text{cm}^{-3}$$

$$B_{ss} = 0.28B_{bs} = 0.28 \times 220\mu\text{G} = 62\mu\text{G}$$

evolution of double power law:

$$n(\gamma, t) = \min[n_1(p_1, \gamma, t), n_2(p_2, \gamma, t)]$$

calculate radio synchrotron emissivity in radio lobe

$$\epsilon_\nu d\nu = -\frac{dE}{dt} \cdot n(\gamma, t) \cdot \frac{d\gamma}{d\nu} d\nu$$

$$\nu \approx \gamma^2 \nu_g \quad \text{where} \quad \nu_g = \left(\frac{e}{2\pi mc}\right) B$$

$$\epsilon_\nu = \frac{4}{3}\sigma_T \gamma^2 c u_B \cdot n(\gamma, t) \cdot \frac{1}{2(\nu\nu_g)^{1/2}}$$

local field

$$\gamma = \gamma(\nu) = \left(\frac{\nu}{\nu_g}\right)^{1/2}$$

radio synchrotron emissivity profiles observed in Cygnus A at 1.345 GHz along boundary backflow

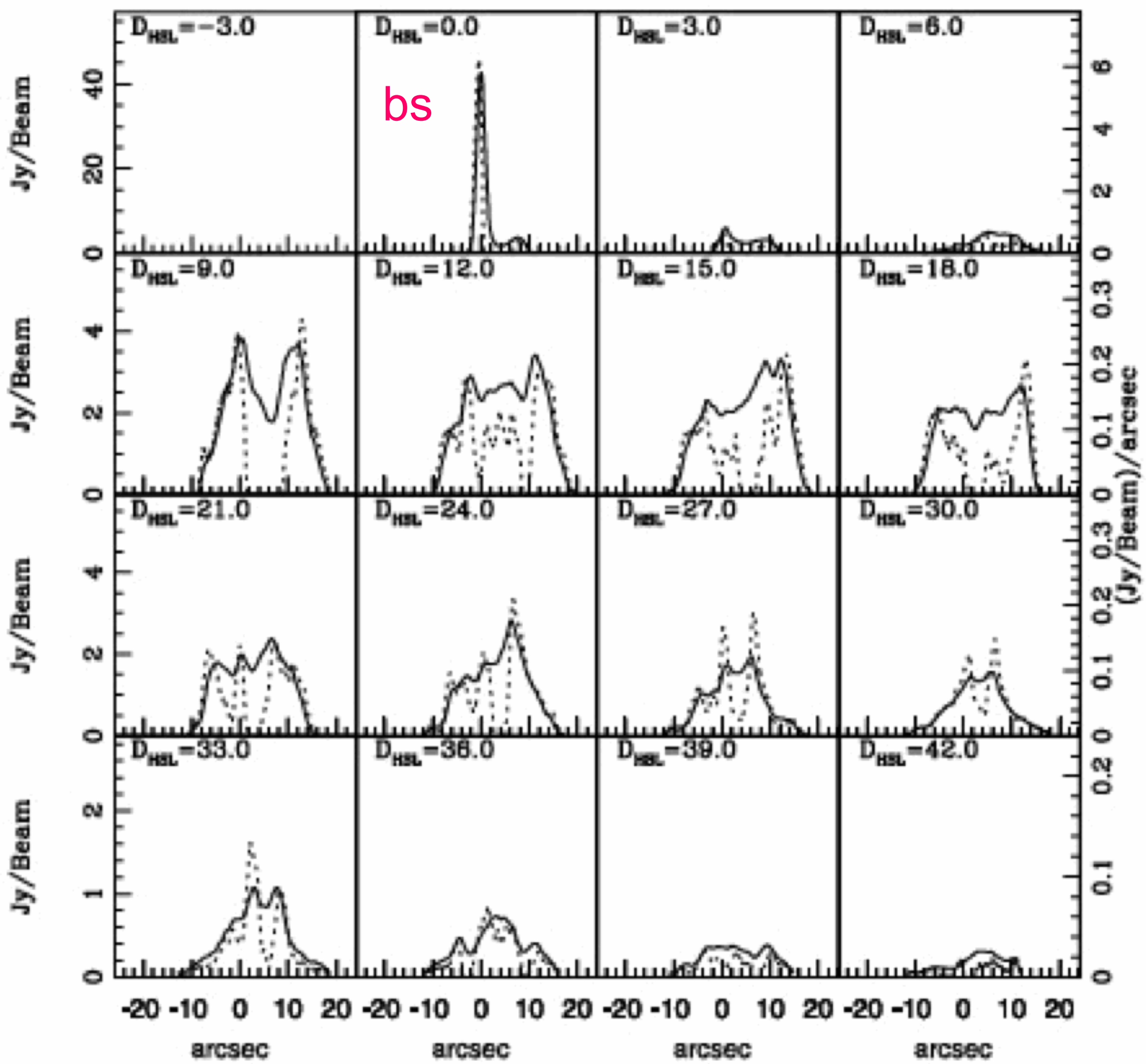

solid lines:
flux profiles

dashed lines:
emissivity profiles

Carvalho+05

computed radio synchrotron emissivity profiles for toroidal B:

emissivity at 1.345 GHz at various z (kpc)

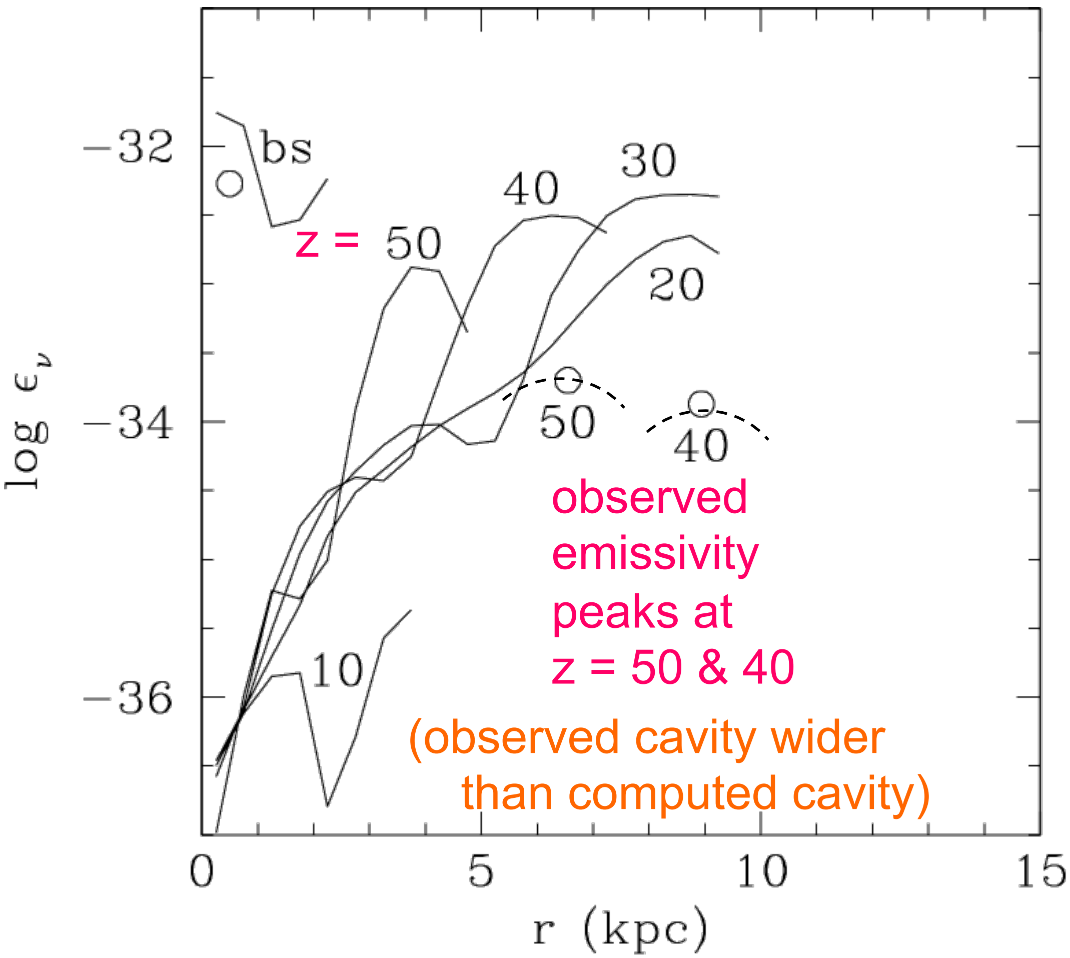

spectra at max $\varepsilon_{1.345}$

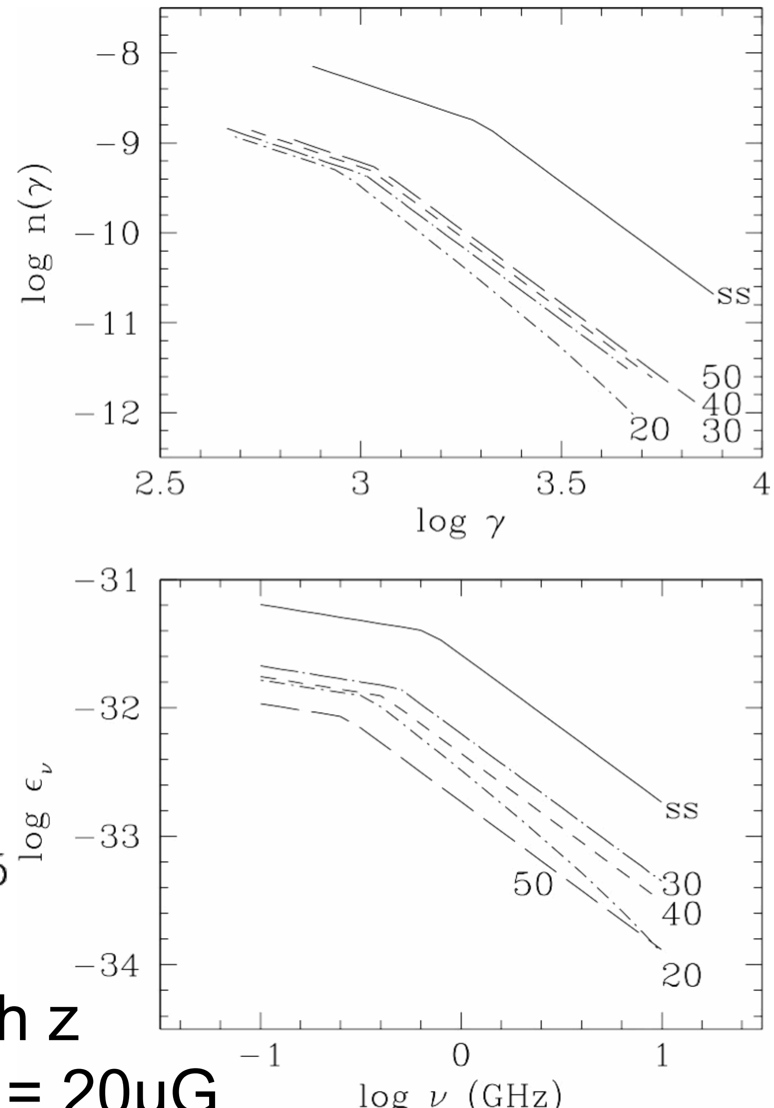

a poor fit: emissivity increases with z

B ~ 100-150μG >> B_{obs} = 20μG

computed radio synchrotron emissivity profiles for random B:

$B_{ran} = B_{ss}(\rho/\rho_{ss})^{2/3}$

emissivity at 1.345 GHz at various z (kpc)

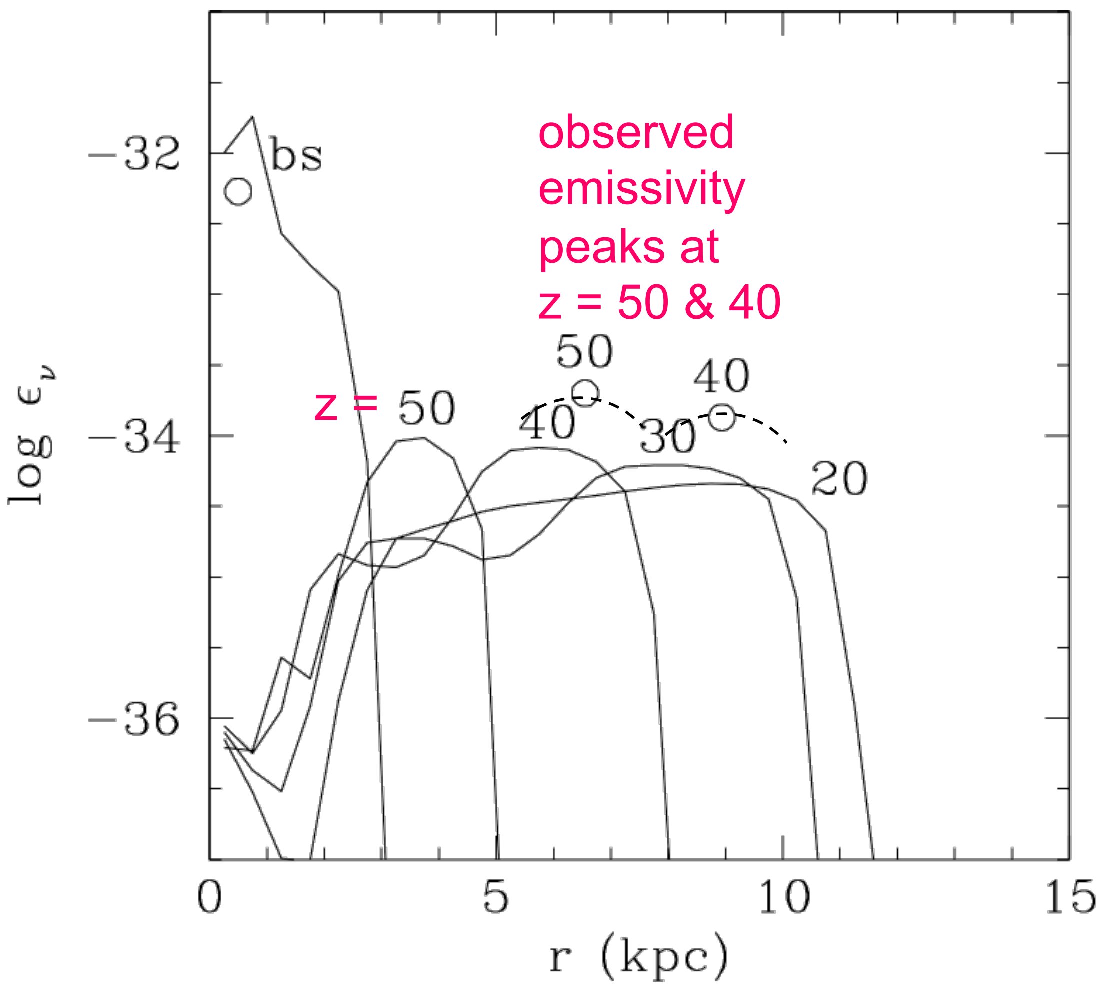

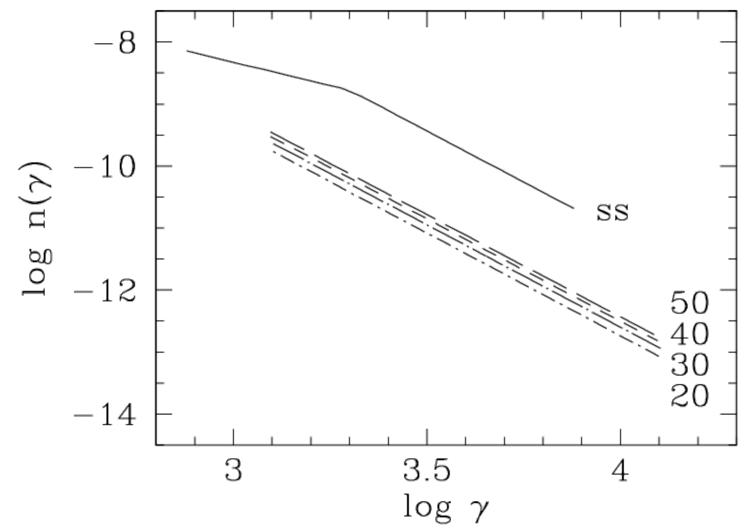

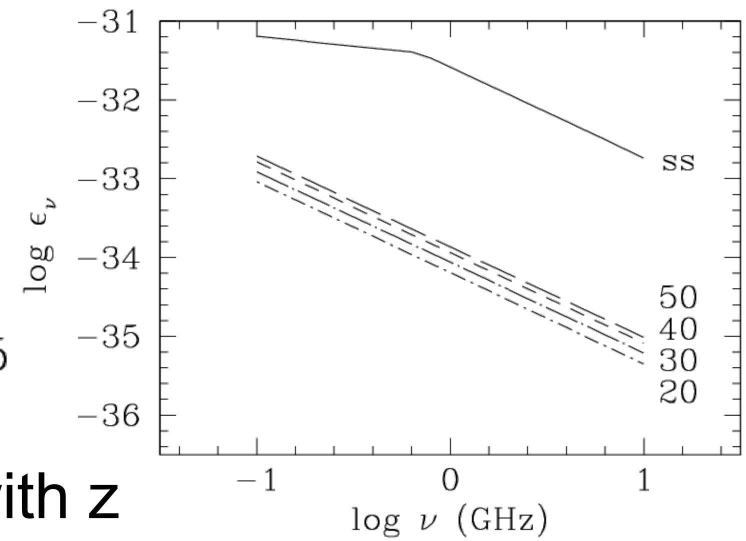

a good fit: emissivity decreases with z and B = 20μG = B_{obs} = 20μG computed radio synchrotron emissivity profiles for random B:

$B_{ran} = B_{ss}(\rho/\rho_{ss})^{2/3}$

emissivity at 1.345 GHz at various z (kpc)

solution 1

$L_{cr} = 10^{46}$ erg/s and $V_{cav} = 0.2V_{obs}$:

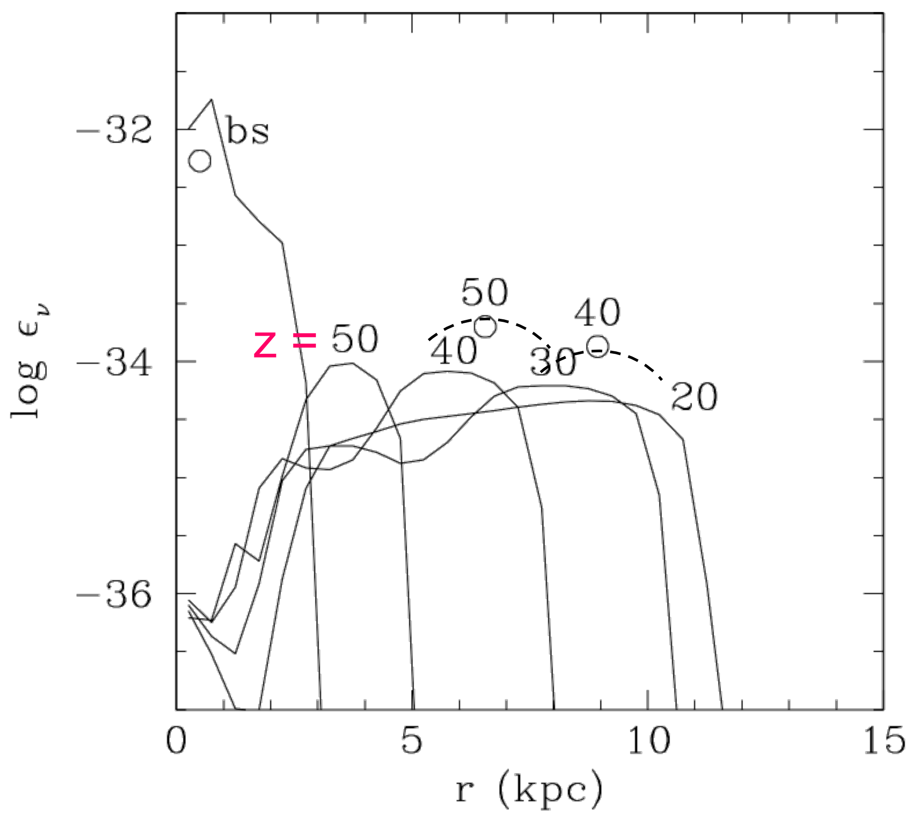

solution 2

$L_{cr} = 2.6 \times 10^{46}$ erg/s and $V_{cav} = V_{obs}$:

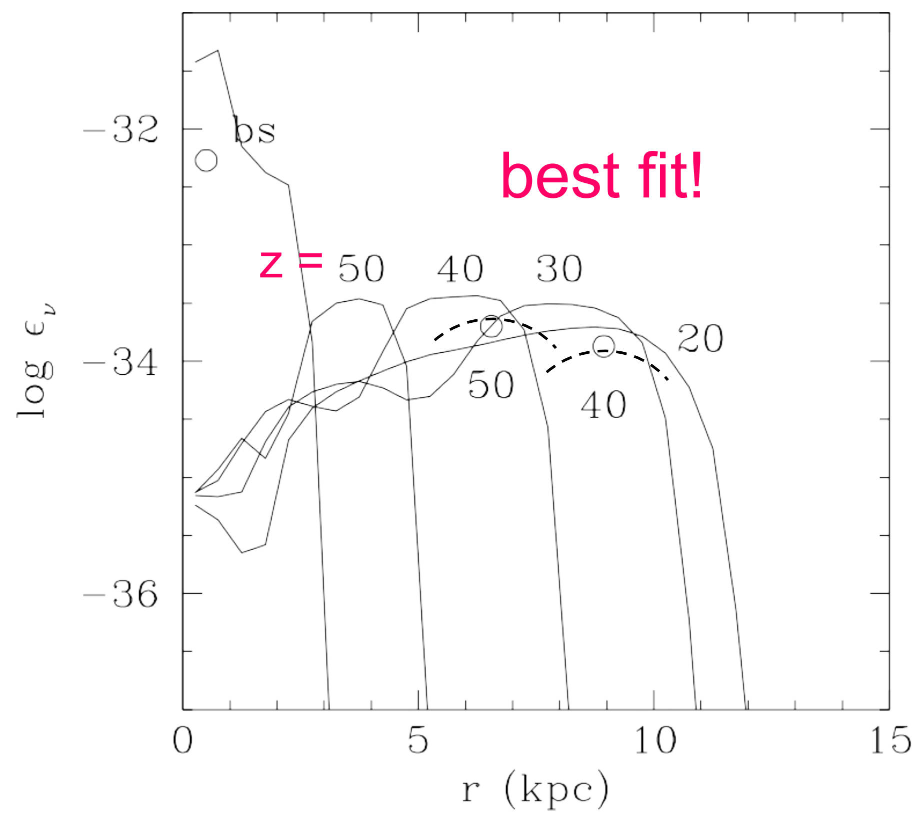

random B implies subgrid (sub-kpc) field structure best evidence yet for electron-pair dominance in FRII jets :

Solution 2 $L_{cr} = 2.6 \times 10^{46}$ erg/s and $V_{cav} = V_{obs}$:

Find current energy density of radiating electrons in shock spot from energy density observed in bright spot:

$$e_{c,ss,rad} = m_e c^2 \int_{\gamma_{min}}^{\infty} \gamma n_{ss}(\gamma) d\gamma \approx \boxed{2.9\text{–}2.5 \times 10^{-8} \ \text{erg cm}^{-3}}$$

for (unobserved) cutoff energy $\gamma_{min} = 1 - 100$

Here $n_{ss} \propto K$ with

$$K = K_{ss} = \frac{\langle e_{c,ss}\rangle}{\langle e_{c,bs}\rangle} K_{bs,obs} = 2.31 K_{bs,obs} \quad \text{erg cm}^{-3}$$

Dynamically computed ss energy density at time 10 Myrs:

$$\boxed{e_{c,ss} \approx 2.5 \times 10^{-8} \ \text{erg cm}^{-3}}$$

all relativistic particles in the shock spot are electron-pairs, consistent with an electro-magnetic origin of the jet

more conclusions:

- Accurate calculation of radio synchrotron everywhere inside the radio lobe from observed energy spectrum in brightspot ("hotspot")
- toroidal (and B_r) fields resolved by the ~kpc grid increase exponentially along the backflow, exceeding the observed field and with too much radio emission
- subgrid (sub-kpc) scale random fields have uniform fields similar to those observed (B ~ 20 μG) and radio synchrotron emission that agrees with observations
- the energy density of radiating relativistic electrons in the post-shock region agrees with the energy density required to inflate the Cygnus A cavity --- this indicates that the jet is also dominated by relativistic electron pairs